Proceedings of ASME Turbo Expo 2011
GT2011
June 6-10, 2011, Vancouver, British Columbia, Canada

GT2011-45250

INVERSE FIN ARRANGEMENT IN A LOW PRESSURE TURBINE TO IMPROVE THE INTERACTION BETWEEN SHROUD LEAKAGE FLOWS AND MAIN FLOW

Inga Mahle and Roman Schmierer
MTU Aero Engines GmbH
Munich, Germany

ABSTRACT

The paper deals with the geometry of the shroud cavities in low pressure gas turbines and presents a design which helps to reduce the losses that arise when the shroud leakage flows interact with the main flow.

The fins in low pressure gas turbines are usually attached to the shroud of the blades. They are therefore rotating while the non-rotating honeycomb or abrasive coating is mounted into the casing. The shroud leakage flow, after passing the rear fin, is decelerated in the rear cavity chamber and enters the main flow path with an axial velocity that is smaller than the axial velocity of the main flow. This difference in axial velocity, together with differences in the circumferential velocity, leads to increased turbulence, mixing losses and an unfavorable incidence of the subsequent vane row in the wall region.

Contrarily to the usual configuration, the inverse fins in the turbine presented in the paper are attached to the casing while the honeycomb is mounted onto the rotating blades. This arrangement results in the location of the gap between the fin and the honeycomb being very close to the position of re-entry of the leakage flow into the main flow. Therefore, the leakage flow keeps a high velocity resulting from the narrow fin gap until re-entry which reduces the velocity difference with respect to the main flow. Consequently, the mixing losses and subsequent row losses are reduced. Due to the favorable position of the gap and a particular shaping of the honeycomb, the leakage flow is kept close to the surface of the shroud and enters the main flow with little perturbations.

The paper presents numerical results of steady 3D simulations of a three-stage low pressure turbine. Results with an ideal flow path (no cavities), with shroud cavities with conventionally rotating fins and with shroud cavities with inverse fins are compared.

NOMENCLATURE

C	[-]	non-dimensional absolute velocity
h	[-]	non-dimensional enthalpy
H	[-]	non-dimensional flow path height
m	[-]	non-dimensional mass flow rate
tke	[-]	non-dimensional turbulent kinetic energy
y^+	[-]	non-dimensional wall distance
α_Z	[°]	flow angle in x-Φ-plane
ε_Z	[°]	flow angle in x-r-plane
η	[-]	isentropic efficiency

Subscripts

L	leakage flow
M	main flow
r	radial
x	axial
Φ	circumferential

INTRODUCTION

Endwall losses due to leakages represent one of the major loss sources in modern gas turbines. It is therefore of great interest to understand and reduce these losses which are caused by the leakage flows through the inner rim seal and the outer shroud cavities. Gier et al. [1] presented a loss breakdown for inner and outer cavities based on CFD simulations and measurements for a three-stage, low pressure turbine. The authors highlighted the particular importance of the mixing losses at re-entry of the leakage flows into the main flow and of the subsequent row losses which consist of incidence and secondary-flow losses in the subsequent blade rows.

Especially the impact of shroud leakage flows, i.e. leakage flows that are passing through the outer cavities above the rotating blades, on main flow have been subject to a number of experimental and numerical investigations, e.g. Anker & Mayer [2], Pfau et al. [3], Giboni et al. [4], Peters et al. [5]. These authors mainly agree in their conclusions, namely that the leakage flow increases the mixing losses and impacts the secondary flow in the subsequent blade rows. They also show that the negative incidence of the downstream stator which is caused by the difference in flow direction of leakage flow and main flow is harmful and can lead to a flow separation on the downstream stator.

A range of investigations is also dedicated to geometry modifications of shroud cavities and their consequences for the interaction between leakage flows and main flow. Examples are variations of clearances, e.g. Peters et al. [6] and of shroud geometries, e.g. Rosic et al. [7]. Even though some modifications present a considerable improvement in mixing losses and other harmful effects, like the ingress of main flow fluid in the cavity, not all of them are realizable in the turbines of flight engines. One main reason is that such engines often require certain axial and radial gaps due to the expected movement of the rotor relative to the casing.

Some elaborate geometrical modifications that can be found in literature directly aim at reducing mixing losses and subsequent row losses by influencing the velocity components of the leakage flow.

In a numerical and experimental study of a four-stage, low aspect ratio turbine, Wallis et al. [8] investigated the effects of a turning device in the form of tiny bladelets fixed onto the rotor shroud immediately downstream of the radial fin. The bladelets are supposed to alter the circumferential velocity of the flow exiting the cavity in order to reduce the mixing losses. However, even with a modification of the fin arrangement, only a decrease in efficiency could be noted which was attributed to more mainstream flow penetrating into the cavity and re-entering the main annulus with increased swirl. The results improved when adding a series of buffers in the form of flat turning vanes attached onto the casing above the shroud.

The manipulation of the velocity components of the leakage flow was also in the focus of Rosic & Denton [9] who presented experimental results for an outer cavity in a low speed, three-stage turbine. The authors showed a significant improvement in flow angle and loss in the downstream stator row by fixing a series of turning vanes onto the casing wall close to the downstream edge of the shroud exit cavity. In contrast to Wallis et al. [8], the turning vanes in [9] are stationary. They turn the leakage flow into the direction of the main passage flow which reduces the mixing losses.

Schlienger et al. [10] presented measurements based on geometrical variations of shroud cavities in a low speed, two-stage research turbine. The first geometry included a large rectangular re-entry cavity volume which decelerated the leakage flow after the seal gap. The second geometry of the re-entry cavity was reduced in size and had a spline shaped contour added to the end wall which manipulated the axial and radial velocity of the leakage flow. The authors showed that the gas path of the leakage jet and the incidence angles on the downstream blade row changed by the geometrical modification. However, no beneficial effect on overall turbine efficiency was found.

Modifications of the re-entry cavity by inserts were also investigated numerically and experimentally by Rosic et al. [11] in a three-stage high pressure steam turbine. The authors studied three different concepts: a profiled exit cavity downstream end-wall, an axial deflector and a radial deflector. Improvements of the flow in the subsequent stator row were due to a reduced radial velocity at the re-entry of the cavity flow into the main flow and to a shift of the point of re-entry in the upstream direction. Together with a reduction of main passage fluid ingress into the cavity, these improvements led to considerable increases in measured and simulated turbine efficiency.

Similar improvements over a conventional fin arrangement are noted for the inverse fins that are under numerical investigation in this paper. Even though the necessary attachment of the honeycomb or abrasive coating on the rotor is technically challenging, the concept has the advantage of not imposing any limits to the rotor axial movement.

The usage of inverse fins is not a complete novelty. They can often be found in stationary steam turbines and various geometrical modifications have been studied previously, e.g. Bohn et al. [12]. However, to the authors' knowledge, no investigation has been published so far which compares directly conventional and inverse fins in the turbine of a flight engine like this paper does.

The paper is divided in different sections. In the first section, the test cases, i.e. the turbine with and without cavities, are presented and important aspects of the numerical simulation are highlighted. The next section is about the impact of the leakage flow from cavities with conventional fin arrangement. Streamlines and radial distributions of important flow quantities from simulations with and without cavities are compared. In the final sections, the impacts of the inverse fin arrangement are presented and the improvement of the interaction between main and leakage flows is investigated.

TEST CASE

The turbine under investigation in this CFD study is a three-stage, low pressure turbine. A predecessor of this turbine has been used in the investigation of Gier et al. [1] which differs from the turbine under investigation by the shape of the duct and the blading but has the same design operating point and turbine power.

Figures 1 and 2 show the main annulus of the turbine without any cavities as well as without any tip clearances and with outer cavities as used for the present investigation. Since the aspect ratio of the turbine is sufficiently large (larger than 3 for all blades), there is no interaction between the leakage flows from the outer and inner cavities when the latter ones are present. Therefore and since this study is focused on the outer cavities, the inner cavities are not included in the CFD model. The size of the radial gaps is about 0.55% of the respective blade height. In the following, the outer cavity situated above the blade of the first stage is denoted by Cav1, the cavity above the blade of the second stage Cav2 and the one above the blade of the third stage by Cav3 (Fig. 2).

NUMERICAL METHOD

The simulations are performed with the code TRACE, a 3D compressible Navier-Stokes code based on a block-structured finite volume scheme. Diffusive fluxes are computed with a central scheme while for the convective fluxes a higher order MUSCL scheme combined with the flux differencing method of Roe is used. Additionally, these fluxes are limited with a special version of the Van Albada Limiter. Time integration is performed with an implicit procedure until a steady state is reached. Mixing planes with flux averaging and non-reflective interfaces under full mass conservation are used to couple the non-rotating and rotating parts of the turbine.

More details concerning TRACE can be found in [13] where a good agreement between a simulation of a turbine with cavities and measurements is shown.

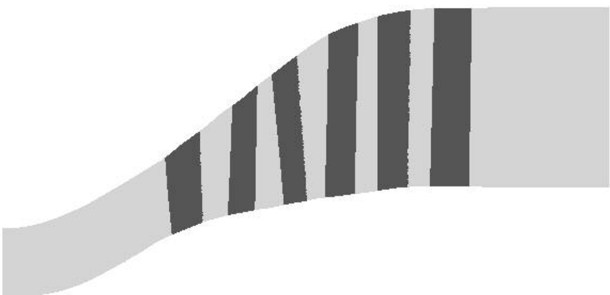

Figure 1: Main annulus without cavities and without tip clearances

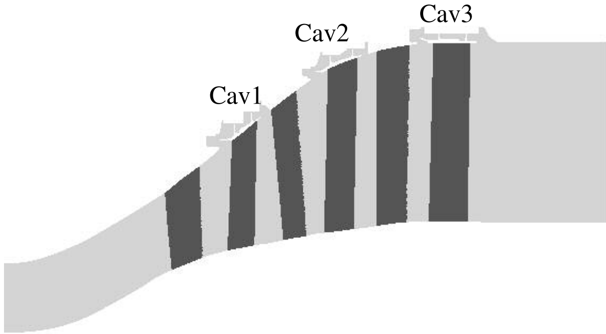

Figure 2: Main annulus with outer cavities Cav1, Cav2 and Cav3

Turbulence and Transition Modeling

In order to ensure a reliable representation of turbulence in the boundary layers for Reynolds numbers that are typical for jet engines, a k-ω two equation model is used in TRACE. While a low-Reynolds number approach is taken for the blade surfaces, wall functions are applied for the end walls and within the cavities. Since the present analysis focuses on the mixing process between the cavity flow and the main flow, the capturing of the very small flow structures in the cavities is believed to be of second importance only. More details and references concerning turbulence and transition modeling in TRACE can be found in [1].

Mesh Generation

Structured grids are used for both, the main annulus and the cavities. However, main annulus and cavity grids are first generated separately. Then they are assembled with the help of interfaces.

Cavities

The mesh of the cavities is created with the grid generator Icem Hexa. The grid is first defined in the 2D plane of the cross section and then extended in the pitch wise direction. Figure 3 shows such a 2D grid before extension in the third direction. Grid refinements in zones with high gradients, e.g. around the fins, ensure that their resolution is sufficient.

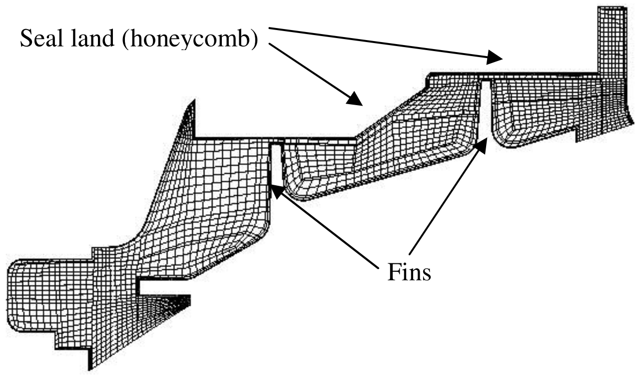

Figure 3: Grid of Cav2 with conventional fins. Every third grid point is shown

Main annulus

The grid within each passage of the turbine consists of a structured multiblock mesh with nine blocks created by G3DMesh. An O-grid surrounds each vane or blade while the main part of the channel is gridded with H- and G-topologies.

Merging process and definition of intersections

Within the main flow annulus and the cavities, mixing planes are used to connect sections with different rotational speed and different pitches. When grids with the same rotational speed and the same pitch have to be connected, e.g. the cavities to the main annulus, zonal interfaces are used, which interpolate the aerodynamic data on both sides.

Grid resolution

The total number of points in the main annulus is about 5.1 million while 4.3 million points are used within the cavities with conventional fins and 3.6 million with inverse fins. Regions with high gradients are more finely resolved than others. The number of cells within the radial clearances is the same for the test cases with conventional fins and with the inverse fins. There are about 4000 cells per passage within each radial gap. At the cavity and end walls the dimensionless wall distance y^+ is well within the limits that are suitable for wall functions. A number of refinement studies has been performed in order to ensure that all phenomena that are important for this investigation are well resolved.

Within the O-grids surrounding the blades and vanes, the points are clustered towards the wall so that the dimensionless wall distance y^+ is about 1 and a low-Reynolds number approach can be used.

Boundary Conditions

At the inlet and outlet of the computational domain, non-reflecting boundary conditions are used. The radial distributions of total pressure, total temperature and flow angles are taken from experimental results obtained with the predecessor of the present turbine. The turbulence intensity at the inlet is low because of the specific rig test conditions.

All walls are assumed to be adiabatic with the velocity set to zero at fixed walls and set to the correct rotational velocity at rotating walls. More details concerning boundary conditions can be found in [1].

Convergence

The simulations were accepted to be converged when mass flow, pressure ratio and efficiency of the whole turbine and the individual stages remained constant within very sharp limits and show no oscillations. Additionally, the residuals at convergence had to be at least two orders of magnitude smaller than at the beginning of the simulations.

INTERACTION OF SHROUD LEAKAGE FLOWS AND MAIN FLOW FOR CONVENTIONAL FINS

Figure 3 shows Cav2 with the so-called conventional fin arrangement. The fins are attached to the shroud of the blade, while the seal land made out of honeycomb is mounted in the casing. The conventional fin arrangement is subject of investigation in this section, the inverse fin arrangement shown in Fig. 4 will be dealt with later in the paper.

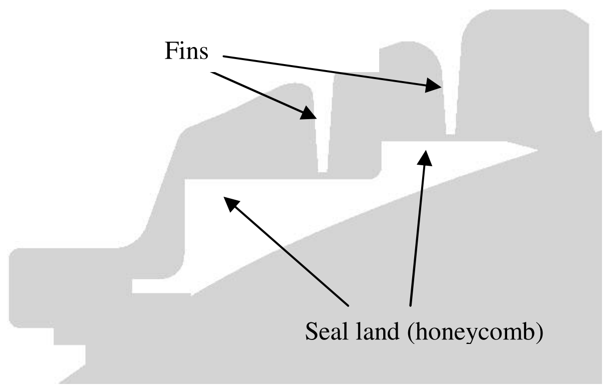

Figure 4: Cav2 with inverse fins

When comparing the results of two steady 3D Navier-Stokes simulations of the turbine under investigation, without (Fig. 1) and with outer cavities (Fig. 2) at the same turbine power, a decrease in isentropic turbine efficiency of 0.87% due to the outer cavities can be noted. A large part of the cavity losses that lead to this decrease in efficiency are the so-called mixing losses. Gier et al. [1] compute them to comprise about 48% of the cavity losses. Another important loss mechanism are the subsequent blade losses, about 13% in the case of Gier et al. [1].

Both, the mixing losses and the subsequent row losses, originate from differences in the respective velocity components of main flow and leakage flow. Figure 5 shows the situation close to the rear opening of a shroud cavity. While the main flow in location A has been turned and accelerated by the precedent blade, the leakage flow has only been influenced by wall friction during its passage through the cavity. Therefore its circumferential absolute velocity component C_Φ is significantly larger than the circumferential velocity component of the main flow which can even be directed in the opposite direction. The different velocity components of main and leakage flow lead to velocity gradients in the region of re-entry which produce turbulence and losses. In addition, the subsequent vane experiences an unfavorable negative incidence in the tip region. Even though the large difference in circumferential velocity component, which has been subject of earlier studies of inner cavities [14], is not reduced by the inverse fin concept, significant improvements are made by reducing the difference in the axial velocity component and changing the way how the cavity flow is inserted into the main flow.

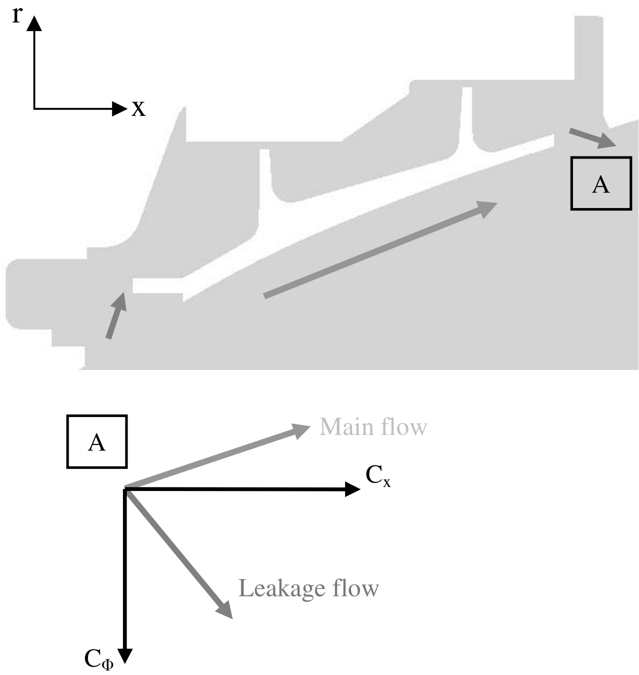

Figure 5: Velocity of main and leakage flows in the region of re-entry A

Figure 6 shows streamlines based on circumferentially flux-averaged quantities in the rear part of the outer cavity Cav2 and in the main flow. It can be seen that the entering of the flow from the shroud cavity into the main flow is not smooth at all and happens in the rear half of the cavity opening. There is even fluid from the main flow entering into the cavity in the front half of the opening and participating in the formation of a vortex in the cavity chamber. The leakage flow acquires a high velocity when passing the fin. However, before it enters the main flow it has traversed the rear cavity chamber where its high velocity is reduced by expansion and becoming unfavorably small in comparison to the main flow which has been accelerated in the blade.

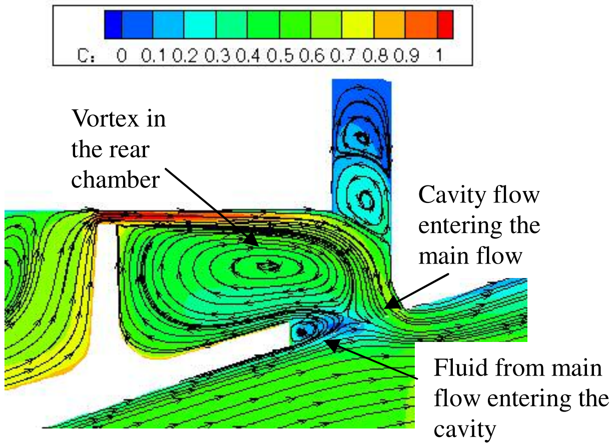

Figure 6: Streamlines and absolute velocity in the rear part of the cavity Cav2 with a conventional fin arrangement and in the main flow

In the following, radial distributions of circumferentially averaged flow quantities are investigated, in order to gain more insight into the differences between the simulations with and without cavities. Figure 7 shows the planes P1 to P3 that are introduced for this purpose at the rear opening of Cav2 and behind the subsequent blade row. P1 is located approximately in the middle of the opening, P2 shortly upstream of its end and P3 behind the subsequent vane row. Even though the modification of the fin arrangement has been applied to all three outer cavities of the turbine, only Cav2 is discussed in the following since the observations that can be made from it are representative of all three cavities. All quantities in the following, including those in figures and tables, are normalized by the velocity and the mass flow at the entry of the turbine.

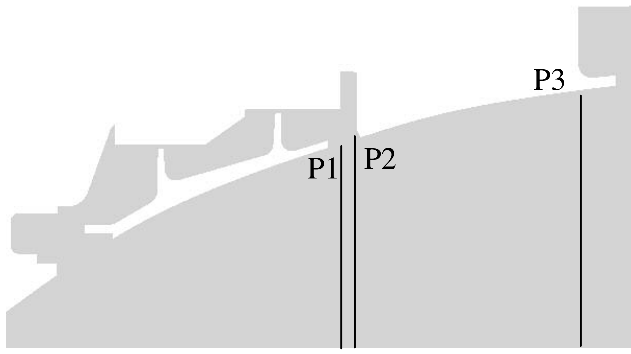

Figure 7: Planes P1 to P3 for Cav2

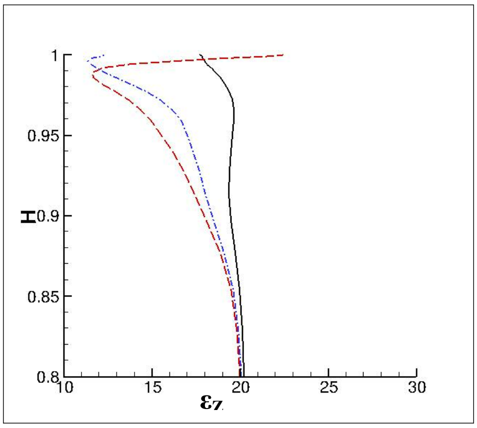

Figure 8: Radial distribution of angle ε_Z in P1, averaged in circumferential direction, solid black line: without cavities, dashed red line: with cavities and conventional fins, dashed-dotted blue line: with cavities and inverse fins

Figure 8 shows the angle in the x-r-plane

$$\tan \varepsilon_Z = C_r / C_x \qquad (1)$$

over the non-dimensional flow path height H in P1. For clarity only the upper 20% of the height are shown. The solid black line in Fig. 8 is the result of a simulation without cavities. The dashed red line is the result of a simulation with outer cavities with conventional fins. The inverse fins are included in the simulation which led to the dashed-dotted blue line and is subject of statements later in this paper.

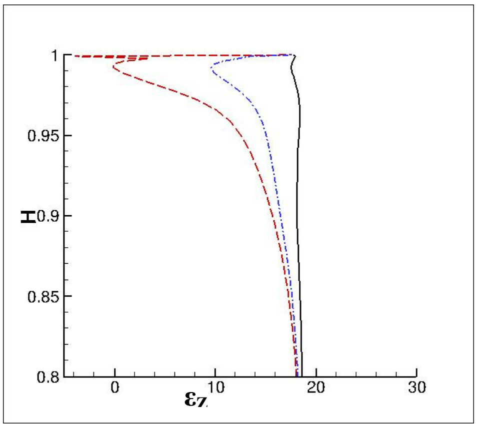

Figure 9: Radial distribution of angle ε_Z in P2, averaged in circumferential direction, lines as in Fig. 8

When comparing the radial distributions of ε_Z without cavities and with conventional fin cavities in Fig. 8 it becomes clear that fluid from the main flow is entering the cavity at this location (P1) since the angle with cavities in the tip region is larger than the angle without cavities. This is in agreement with the streamlines in Fig. 6. In P2 ε_Z with conventional fin cavities is smaller than without (Fig. 9). This indicates that the flow in P2 is directed from the cavity into the main flow.

The radial distribution of the circumferential velocity component C_Φ confirms that the fluid from the conventional fin cavity is entering the main flow only in the second half of the cavity opening: While there are little differences in the radial distribution between the two results in P1 (Fig. 10), the circumferential velocity component in the tip region in P2 (Fig. 11) is clearly larger with cavities than without. This comes from the fact that the fluid that has passed through the cavity has hardly experienced any turning compared to the direction it had when entering the cavity while the main flow has been turned by the blade.

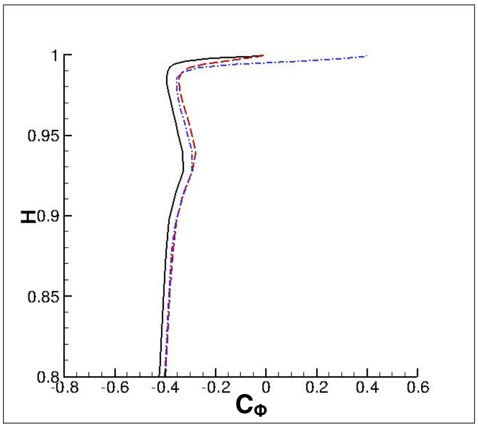

Figure 10: Radial distribution of circumferential velocity in P1, averaged in circumferential direction, lines as in Fig. 8

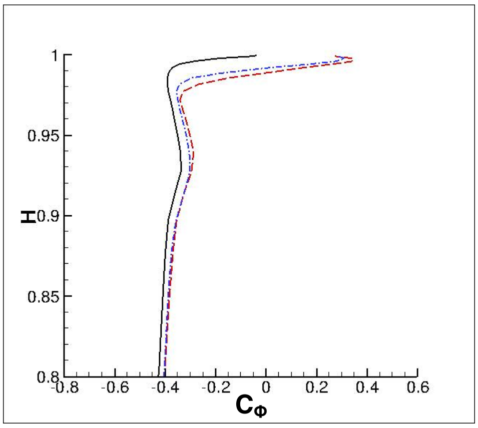

Figure 11: Radial distribution of circumferential velocity in P2, averaged in circumferential direction, lines as in Fig. 8

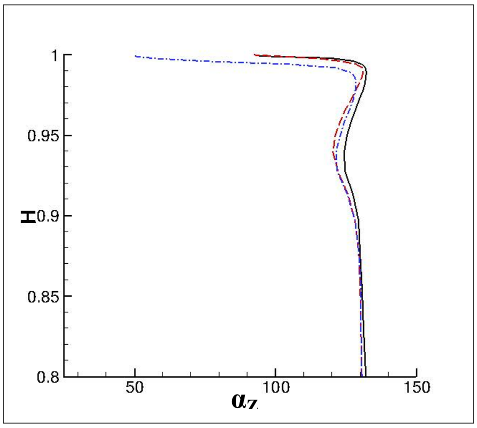

Figure 12: Radial distribution of flow angle in P1, averaged in circumferential direction, lines as in Fig. 8

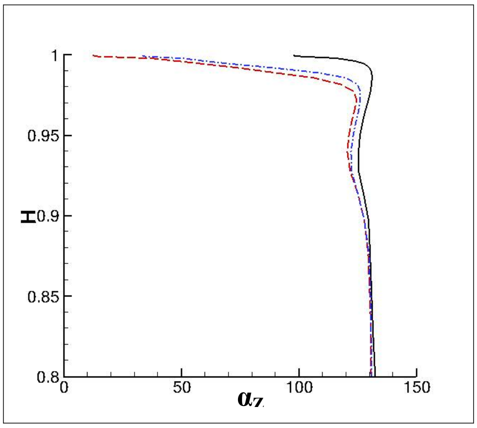

Figure 13: Radial distribution of flow angle in P2, averaged in circumferential direction, lines as in Fig. 8

Different circumferential and axial velocity components also lead to a different flow angle

$$\tan \alpha_Z = C_x / C_\Phi \tag{2}$$

As it is to be expected from the preceding observations, the difference in flow angle between the results with and without cavities in the tip region is much more pronounced in P2 (Fig. 13) than in P1 (Fig. 12). This is another consequence of the relatively late entry of the cavity flow into the main flow. Figure 13 shows a clearly visible decrease in flow angle by the cavities compared to the result with an ideal flow path down to 97% of the flow path height. If this change in flow angle due to the leakage flow is not taken into account when designing the subsequent vane, losses due to a non-ideal, negative incidence angle occur. Figure 14 shows that this is the case in the turbine under investigation: a region with reverse flow forms in the tip region on the pressure side of the third vane when the conventional fin cavities are present (Fig. 14b vs. 14a).

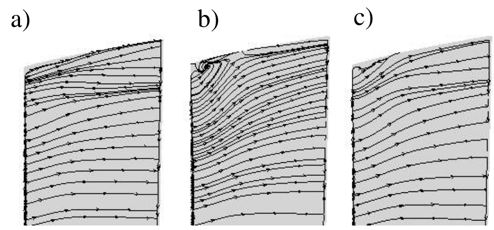

Figure 14: Streamlines on the upper 25% of the pressure side of the third vane. a) without cavities, b) with cavities and conventional fins, c) with cavities and inverse fins

An increased turbulence caused by the mixing of main and leakage flows can be seen in Fig. 15 for P2 and in Fig. 16 for P3. Both figures show the radial distribution of turbulent kinetic energy (tke). In P2, the test case with conventional fin cavities shows a single peak of tke at approximately 98.5% flow path height. In P3, the peak of the turbulent kinetic energy with cavities is not as pronounced as in P2 due to the mixing that has occurred between the two locations. However, the difference between the two results extends down to 85% flow path height and therefore influences more than just the tip region.

All radial distributions of flow quantities shown in this section demonstrate large differences between the cases with conventional fin cavities and without cavities in the wall region. These differences lead to a substantial increase in losses and a decrease in turbine efficiency. In the following it is investigated how a different fin arrangement which changes the way how the cavity flow enters into the main flow can improve the situation.

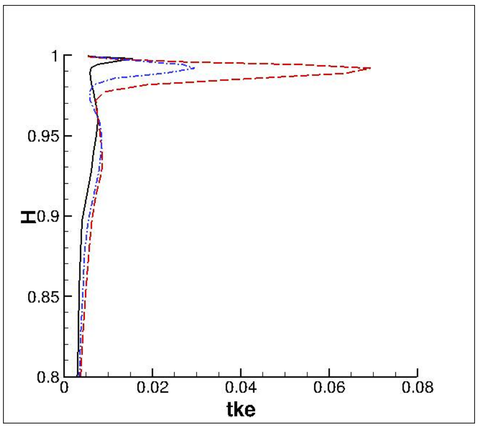

Figure 15: Radial distribution of turbulent kinetic energy in P2, averaged in circumferential direction, lines as in Fig. 8

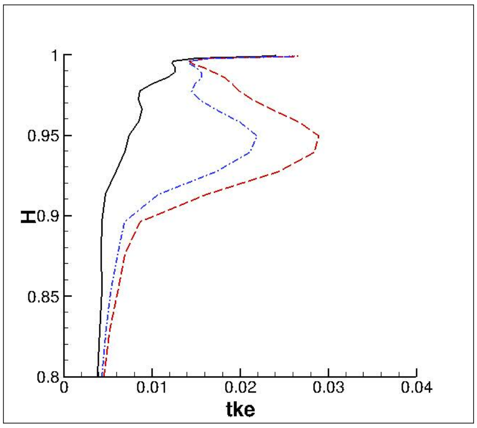

Figure 16: Radial distribution of turbulent kinetic energy in P3, averaged in circumferential direction, lines as in Fig. 8

IMPROVEMENT BY AN INVERSE FIN ARRANGEMENT

Contrarily to the usual configuration (Fig. 3), the inverse fins are attached to the casing and therefore are non-rotating. The seal land made out of honeycomb is mounted onto the rotating blades (Fig. 4) . It has an inclined surface towards its rear end.

When exchanging the usual fin configuration by the inverse one and keeping the power of the turbine constant by adapting the exit pressure, an increase in isentropic turbine efficiency of 0.14% can be noticed. This means that 16% of the cavity losses, which account for a decrease of 0.87% in isentropic turbine efficiency, have been recovered. With the mass flows through the cavities only changing by less than 2% due to the same radial clearance, most of the increase in turbine efficiency can be attributed to a more favorable mixing between the shroud leakage flow and the main flow and a reduction of subsequent blade losses. Since the present analysis is done on a delta basis between the two very similar configurations of the turbine that only differ by the fin arrangement, an efficiency improvement of 0.14% can be predicted with confidence. Due to this increase in efficiency at the same turbine power, the pressure ratio is smaller by 0.47% for the configuration with the inverse fins.

Figure 17 shows the radial distribution of the overall isentropic turbine efficiency for a simulation without cavities (solid black line), with outer cavities with conventional fins (dashed red line) and with outer cavities with an inverse fin arrangement (dashed-dotted blue line) for the upper 40% of the main flow path. It can be seen that the cavity losses extend down to 75% of the main flow path. It can also be seen how the inverse fins improve the efficiency and bring the radial distribution closer to the solution without cavities.

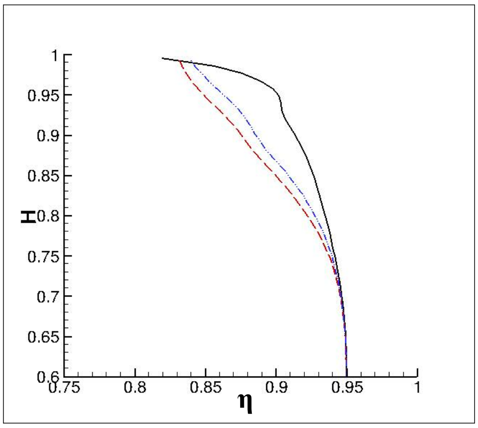

Figure 17: Radial distribution of overall isentropic turbine efficiency, lines as in Fig. 8

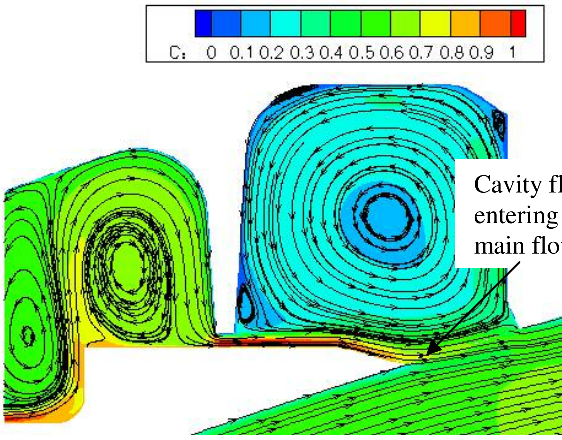

Figure 18: Streamlines and absolute velocity in the rear part of the cavity Cav2 with an inverse fin arrangement and in the main flow

Figure 18 shows streamlines in the rear part of the outer cavity Cav2 with inverse fins. The entering of the flow from the shroud cavity into the main flow happens much smoother than with conventional fins (Fig. 6). On the average, the cavity flow enters the main flow and not vice versa. While the cavity flow with conventional fins enters the main flow in the rear half of the cavity opening, the entering of the cavity flow into the main flow with inverse fins mainly happens in the front half of the opening. Since this location is closer to the fin gap where the leakage flow has acquired a high velocity, it is expected that the speed of the leakage flow at re-entry for the configuration with inverse fins is higher than the speed of the leakage flow for the conventional fins. That this is indeed the case and leads to a reduction of the mixing losses is shown later in this section.

When comparing the radial distributions of the angle ε_Z in the x-r-plane in P1 with conventional and with inverse fin cavities to the result without cavities (Fig. 8), it can be seen that while the angle in the tip region with conventional fins is larger than the angle without cavities, the one with inverse fins is smaller. This demonstrates that, in the average, the cavity flow with inverse fins is directed out of the cavity into the main flow. In location P2, the angle ε_Z with inverse fins is closer to the result obtained without cavities than the angle with conventional fins (Fig. 9). This indicates a smoother insertion of the leakage flow into the main flow.

The radial distributions of the circumferential velocity component in P1 (Fig. 10) also demonstrate that the shroud leakage flow with inverse fins is already entering the main flow at this location: In the tip region the circumferential velocity with inverse fins differs from the circumferential velocity with conventional fins and without cavities. Figure 12 shows the consequence for the flow angle with inverse fins in P1 which, in contrary to the flow angle with conventional fins, already deviates clearly from the flow angle of the simulation with an ideal flow path.

Figures 11 and 13, which show the circumferential velocity component and the flow angle in location P2, demonstrate that the differences between the two simulations with cavities are much smaller in this location than in P1 (Figs. 10 and 12). This is to be expected since the shroud leakage flow in both simulations has completely entered the main flow at this location. However, due to a more upstream entry the cavity flow from inverse fin cavity has mixed better with the main flow when it reaches P2 than the cavity from the conventional fin cavity. Therefore, the negative incidence on the subsequent vane is reduced (Fig. 13) and the reverse flow in the tip region on its pressure side has nearly vanished (Fig. 14c).

That the insertion of the cavity flows happens in a less harmful way with inverse fins than with conventional fins can be also seen from the radial distribution of the turbulent kinetic energy in locations P2 and P3 (Figs. 15 and 16): The peak in turbulent kinetic energy with cavities in location P1 has less than half the height when improving the cavities by the inverse fin arrangement and it is reduced by about a third in location P2.

A major contribution to the reduction in turbulence kinetic energy with the inverse fins is due to a reduction of mixing losses which are evaluated in the following. To estimate the mixing losses, a formula of Denton [15] for the mixing losses within a blade or vane row is used:

$$\Delta h_{mix.row} = \frac{m_L}{m_M}\left[C_{\Phi M}^2\left(1-\frac{C_{\Phi L}}{C_{\Phi M}}\right)+C_{xM}^2\left(1-\frac{C_{xL}}{C_{xM}}\right)\right] \quad (3)$$

Velocities and mass flows of the main flow are denoted with the index M while quantities of the leakage flow have the index L. Since the differences in axial and circumferential velocity components between main and leakage flow are much larger than the differences in radial velocity component, the latter ones are neglected. The values for the main flow are taken from the circumferentially averaged results of a simulation with outer cavities at a non-dimensional flow path height of 94% in P1 and in corresponding planes for Cav1 and Cav3. These locations are well within the region down to which the cavity flows mix with the main flow. The values for the leakage flow are averaged over the rear cavity opening. Taking the main flow values from other non-dimensional flow path heights which are situated in the same region leads to only slightly different results.

	Cav1	**Cav2**	**Cav3**
$C_{\Phi L}$ [-]	0.322	0.448	0.386
$C_{\Phi M}$ [-]	-0.221	-0.279	-0.261
C_{xL} [-]	0.119	0.147	0.104
C_{xM} [-]	0.369	0.480	0.778
m_L [-]	0.008	0.007	0.005
m_M [-]	0.992	0.993	0.995

Table 1: Velocity components and mass flow of main and leakage flows from a simulation with conventional fins

Table 1 shows the individual values for the simulation with conventional cavities, Table 2 for the simulation with cavities that includes the inverse fin arrangement. The table shows significant differences in the axial and circumferential velocity components of main and leakage flows. The difference in axial velocity is more pronounced in the last stage of the turbine than in the first due to the continuous acceleration within the turbine. These velocity differences between leakage flows and main flow, together with the differences in circumferential and radial velocity components (the latter have been neglected in this evaluation) lead to velocity gradients, turbulence and losses. By comparing Tables 1 and 2, the increase in axial velocity of the leakage flow by the more favorable location of the radial gap of the inverse fins is visible.

	Cav1	**Cav2**	**Cav3**
$C_{\Phi L}$ [-]	0.355	0.416	0.330
$C_{\Phi M}$ [-]	-0.226	-0.294	-0.268
C_{xL} [-]	0.267	0.390	0.322
C_{xM} [-]	0.390	0.484	0.782
m_L [-]	0.008	0.007	0.005
m_M [-]	0.992	0.993	0.995

Table 2: Velocity components and mass flow of main and leakage flows from a simulation with inverse fins

Comparing the results from (3) for the two fin arrangements, a reduction of the mixing losses by nearly 40%

by the inverse fins can be noted and attributed mainly to the increase in axial velocity.

CONCLUSIONS

In this paper, the effects of outer cavities on the flow in a three-stage, low pressure turbine have been investigated numerically. The results of simulations with cavities including two different fin arrangements are compared to each other and to the results obtained with an ideal flow path. It is shown that the so-called inverse fin arrangement, with non-rotating fins attached to the casing and a seal land mounted on the blade leads to a more favorable interaction between leakage flow and main flow than a conventional fin arrangement with rotating fins and a fixed seal land. Due to a more upstream entry location of the cavity flow into the main flow, an ingress of main flow fluid into the inverse fin cavity can be avoided. With the fin gap of the inverse fins located closer to the point of entry into the main flow, the difference in axial velocity between leakage and main flow is reduced. So the mixing losses which are a consequence of velocity gradients are decreased by nearly 40%. An additional benefit of the inverse fin cavities which is due to the faster and more upstream entry of the leakage flow into the main flow is that the negative incidence in the tip region of the subsequent vane is reduced and a region of reverse flow, which is clearly visible with conventional fins, is eliminated. Therefore, not only the mixing losses are improved but also the subsequent row losses. In total, the isentropic turbine efficiency with inverse fins is 0.14% higher than with conventional fins.

The promising CFD results of the inverse fin arrangement and the fact that its impact is well visible in the circumferential averaged radial distributions of relevant aerodynamic quantities propose its experimental investigation in a rig test. This is intended for the near future.

ACKNOWLEDGMENTS

The authors wish to thank MTU Aero Engines GmbH for the permission to publish this paper. The partial funding of the work through the Luftfahrtforschungsprogramm Phase 4 is gratefully acknowledged.

The authors also would like to thank Karina Karwan, Anna Musialik, Erik Findeisen and Jonathan Castillo-Reminick for their excellent contribution to this work during their stay at MTU Aero Engines GmbH.

REFERENCES

[1] Gier, J., Stubert, B., Brouillet, B., de Vito, L., 2003, "Interaction of Shroud Leakage Flow and Mainflow in a Three-Stage LP Turbine", ASME Paper GT-2003-38025.

[2] Anker, J. E., Mayer, J. F., 2002, "Simulation of the Interaction of Labyrinth Seal Leakage Flow and Main Flow in an Axial Turbine", ASME Paper GT-2002-30348.

[3] Pfau, A., Schlienger, J., Rusch, D., Kalfas, A. I., Abhari, R. S., 2003, "Unsteady Flow Interactions within the Inlet Cavity of a Turbine Rotor Tip Labyrinth Seal", ASME Paper GT2003-38271.

[4] Giboni, A., Wolter, K., Menter, J. R., Pfost, H., 2004, "Experimental and Numerical Investigation into the Unsteady Interaction of Labyrinth Seal Leakage Flow and Mainflow in a 1.5-Stage Axial Turbine", ASME Paper GT2004-53024.

[5] Peters, P., Menter, J. R., Pfost, H., Giboni, A., Wolter, K., 2005, "Unsteady Interaction of Labyrinth Seal Leakage Flow and Downstream Stator Flow in a Shrouded 1.5 Stage Axial Turbine", ASME Paper GT2005-68065.

[6] Peters, P., Breisig, V., Giboni, A., Lerner, C., Pfost, H., 2000, "The Influence of the Clearance of Shrouded Rotor Blades on the Development of the Flowfield and Losses in the Subsequent Stator", ASME Paper 2000-GT-478.

[7] Rosic, B., Denton, J. D., Curtis, E. M., 2007, "The Influence of Shroud and Cavity Geometry on Turbine Performance – An Experimental and Computational Study, Part 1: Shroud Geometry", ASME Paper GT2007-27769.

[8] Wallis, A. M., Denton, J. D., Demargne, A. A. J., 2000, "The Control of Shroud Leakage Flows to Reduce Aerodynamic Losses in a Low Aspect Ratio, Shrouded Axial Flow Turbine", ASME Paper 2000-GT-475.

[9] Rosic, B., Denton, J. D., 2006, "The Control of Shroud Leakage Loss by Reducing Circumferential Mixing", ASME-Paper GT2006-90946.

[10] Schlienger, J., Pfau, A., Kalfas, A. I., Abhari, R. S., 2003, "Effects of Labyrinth Seal Variation on Multistage Axial Turbine Flow", ASME Paper GT2003-38270.

[11] Rosic, B., Denton, J. D., Curtis, E. M., Peterson, A. T., 2007, "The Influence of Shroud and Cavity Geometry on Turbine Performance – An Experimental and Computational Study, Part 2: Exit Cavity Geometry", ASME Paper GT2007-27770.

[12] Bohn, D., Krewinkel, R., Tümmers, C., Sell, M., 2006, "Influence of the Radial and Axial Gap of the Shroud Cavities on the Flowfield in a 2-Stage Turbine", ASME Paper GT2006-90857.

[13] Yang, H., Nürnberger, D., Kersken, H. P., 2006, "Towards Excellence in Turbomachinery Computational Fluid Dynamics: A Hybrid Structured-Unstructured Reynolds Averaged Navier-Stokes Solver", ASME Journal of Turbomachinery, 128, April, pp 390-402.

[14] Mahle, I., 2010, „Improving the Interaction between Leakage Flows and Main Flow in a Low Pressure Turbine", ASME Paper GT2010-22448.

[15] Denton, J.D., 1993, "Loss Mechanisms in Turbomachines", ASME Paper 93-GT-435.